

Electronic Supporting Information

From molecular to colloidal manganese vanadium oxides for water oxidation catalysis

*B. Schwarz, J. Forster, M. H. Anjass, S. Daboss, C. Kranz and C. Streb**

Institute of Inorganic Chemistry I and Institute of Analytical and Bioanalytical Chemistry, Ulm University, Albert-Einstein-Allee 11, 89081 Ulm, Germany

1. Instrumentation

UV-Vis spectroscopy: UV-Vis spectroscopy was performed on a Shimadzu UV-2401PC spectrophotometer or a Varian Cary 50 spectrophotometer. All systems were used with standard cuvettes ($d = 10.0$ mm).

Thermogravimetric analysis (TGA): TGA was performed on a Setaram Setsys CS Evo, 30 - 1000°C at 10K/min, 50 ml/min air, Graphite crucible 0.5 ml.

Flame atomic absorption spectroscopy (FAAS): Flame atomic absorption spectroscopy was performed on a Perkin Elmer 5100 PC spectrometer.

FT-IR spectroscopy: FT-IR spectroscopy was performed on a Shimadzu FT-IR-8400S spectrometer. Samples were prepared as KBr pellets. Signals are given as wavenumbers in cm^{-1} using the following abbreviations: vs = very strong, s = strong, m = medium, w = weak and b = broad. Comparative IR studies were performed Bruker Tensor 27 FT-IR spectrophotometer including a Platinum ATR unit.

Elemental analysis (EA): Elemental analysis was performed on a Euro Vector Euro EA 3000 Elemental Analyzer as well as on a Elementar vario MICRO cube.

Oxygen evolution quantification: Oxygen concentration in the aqueous phase was measured in a custom-built inert-atmosphere glass vessel in de-oxygenated aqueous solution using a calibrated WTW CellOx 325 Clark-electrode with InoLab 740 measurement system.

Dynamic Light Scattering (DLS): DLS measurements were carried out on a Beckman Coulter Delsa Nano C or a Malvern Zetasizer Nano-ZS using solutions of the catalyst reaction mixture filtered through a hydrophilic syringe filter (0.45 μm). Beckman Coulter Delsa Nano C Detection limits: particle size: 1 – 7000 nm concentration range: 10 ppm –

40 wt-%. Malvern Zetasizer Nano-ZS detection limits: 0.6 nm – 6000 nm; particle concentration detection limit of 0.001 – 1 mass-% (for particles in the 100-1000 nm size range).

Scanning Electron Microscopy (SEM): Scanning electron microscopy was performed on a FEi Helios Nanolab 600 using an acceleration voltage of 20 kV.

Transmission Electron Microscopy (TEM): Transmission electron microscopy was performed on Jeol-1400 transmission electron microscope, Accelerating voltage 120 kV, bright field signal.

Energy dispersive X-ray spectroscopy (EDX): scanning electron microscopy/energy-dispersive X-ray spectroscopy (SEM-EDX) was performed on Hitachi, S-5200 field-emission scanning electron microscope, EDAX Genesis. Double coated conductive carbon tape adhered to the SEM holder from one side and the sample mounted on the other side, then carbon coating of the powder was done to increase the electronic conductivity. 20 kV accelerating voltage was used.

X-ray photoelectron spectroscopy (XPS): XPS was performed on Physical Electronics PHI 5800 spectrometer using monochromatized Al-K α (1486.6 eV) radiation. The measurements were performed with a detection angle of 45°, using pass energies at the analyzer of 93.9 and 29.35 eV for survey and detail spectra, respectively. The samples were neutralized with electrons from a flood gun (current 3 μ A) to compensate for charging effects at the surface.

Nitrogen absorption: Nitrogen absorption isotherms were acquired on a QuadraSorb SI Station 2 – Instrument Version 5.04 at T = 77 K and evaluated using Quantachrome QuadraWin Data Acquisition and Reduction software. Thermal delay was 30 s, outgas time was 1 h, outgas temperature was 350 °C, N₂ was used as adsorbate. Calculation method: de Boer.

Gas chromatography: Oxygen evolution was measured by head-space GC on a Shimadzu GC-2010 gas chromatograph equipped with a 5-Å molecular sieves column and a thermal conductivity detector operated with N₂ carrier gas at 70 °C. Samples (100 μ l) were injected with a gas-tight Hamilton syringe.

Atomic Force Microscopy (AFM): c-AFM measurements were performed in air using a 550 model AFM (Keysight Technologies, USA) with Ti-Pt-coated AFM probes

(ULTRASHARP CSC21/Ti-Pt, μ mash, Bulgaria). The colloid particles were deposited from EtOH dispersion onto a Pt-coated Si wafer (Pt thickness ca. 100 nm).

General remarks: All chemicals were purchased from Sigma Aldrich or ACROS and were of reagent grade. The chemicals were used without further purification unless stated otherwise.

1 Synthesis and characterization of compound 1

1.1 Synthesis of compound 1: $(n\text{-Bu}_4\text{N})_3[\text{Mn}_4\text{V}_4\text{O}_{17}(\text{OAc})_3] \times 3\text{H}_2\text{O}$:

Compound 1 was synthesized and characterized as described in the literature.¹

Elemental analysis for $\text{C}_{54}\text{H}_{123}\text{Mn}_4\text{N}_3\text{O}_{26}\text{V}_4$ in wt.-% (calcd.): C 39.14 (39.21), H 7.38 (7.50), N 2.48 (2.54), Mn 14.15 (13.29), V 13.61 (12.74).

Characteristic IR bands (in cm^{-1} , KBr pellet): 3437 (vb), 2958 (vs), 2933 (vs), 2874 (s), 2359 (w), 2339 (w), 1560 (s), 1481 (vs), 1391 (vs), 1337 (s), 1152 (m), 1026 (w), 968 (s), 947 (vs), 882 (m), 833 (vs), 812 (vs), 779 (vs), 748 (s), 637 (m), 540 (m), 501 (m), 461 (m).

2 Synthesis and characterization of colloid 2

2.1 Synthesis of colloid 2

Colloid 2 was synthesized by sonication ($t = 90$ min, 80 W, room temperature) of 1 ([1] = 0.2 – 1.0 g/L) in de-ionized water.

For bulk analysis of 2, the colloidal particles were precipitated from aqueous solution by the addition of an excess of acetone. The mixture was allowed to stand for one day followed by prolonged centrifugation (4400 rpm). The precipitate obtained was washed with acetone (3x) and was dried. Isolated yield: 22.1 mg (25 wt.-% based on 1)

For subsequent preparative steps for characterization and reactivity see 2.2 – 2.16.

2.2 Dynamic light scattering particle size analysis of colloid 2

Conversion of compound 1 into colloid 2 in pure water was investigated using dynamic light scattering. Statistical analysis of more than 100 single measurements under comparable conditions gave an average particle size of 79 ± 10 nm. Figure S 1 illustrates a representative particle size distribution of 2 obtained by dynamic light scattering. The instrument detection limits are: particle size detection limits: 1 – 7000 nm sample concentration detection limits: 10 ppm – 40wt.-%.

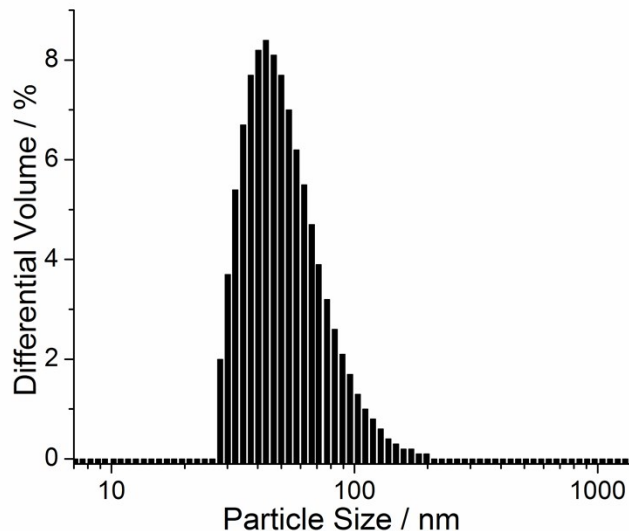


Figure S 1: Volume distribution of colloid **2** gives particles with size between ca. 20 and 200 nm (note: particle size: logarithmic scale).

2.3 Scanning electron microscopy of colloid **2**

Scanning electron microscopy (SEM) of **2** deposited on an Al substrate confirmed the presence of particles in the range of ca. 30 – 190 nm (see Fig. S 2). Particle size was measured using the *ImageJ* software package (<http://rsb.info.nih.gov/ij/>).

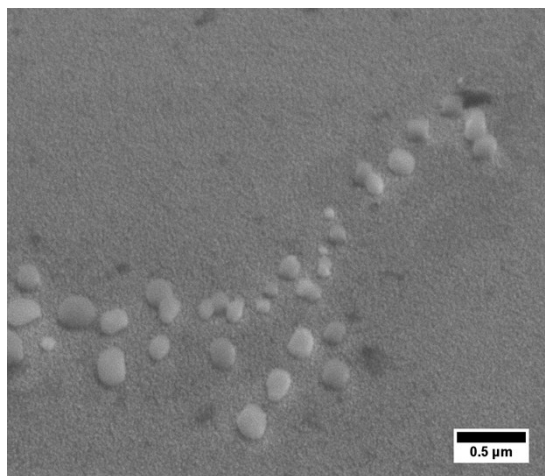


Figure S 2: Scanning electron microscopy (SEM) image of colloid **2**; the section shown is representative of the complete sample.

2.4 Energy dispersive X-ray spectroscopy of colloid 2

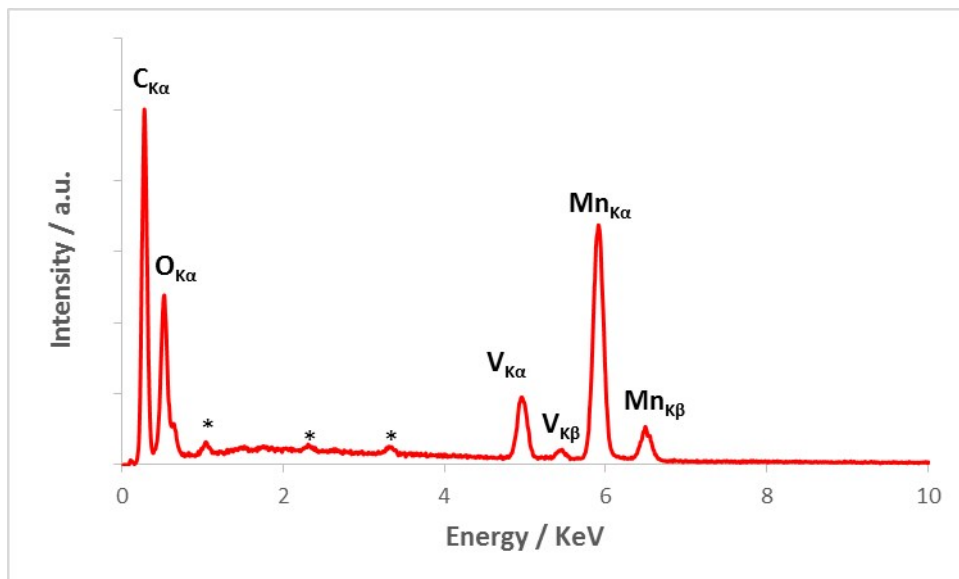


Figure S 3: Energy-dispersive X-ray spectroscopy (EDX) analysis of colloid 2 deposited on carbon substrate showing the presence of the elements Mn, V, O and C. Mn and V are observed in an approximate ratio of 5:1.

2.5 Transmission electron microscopy of 2

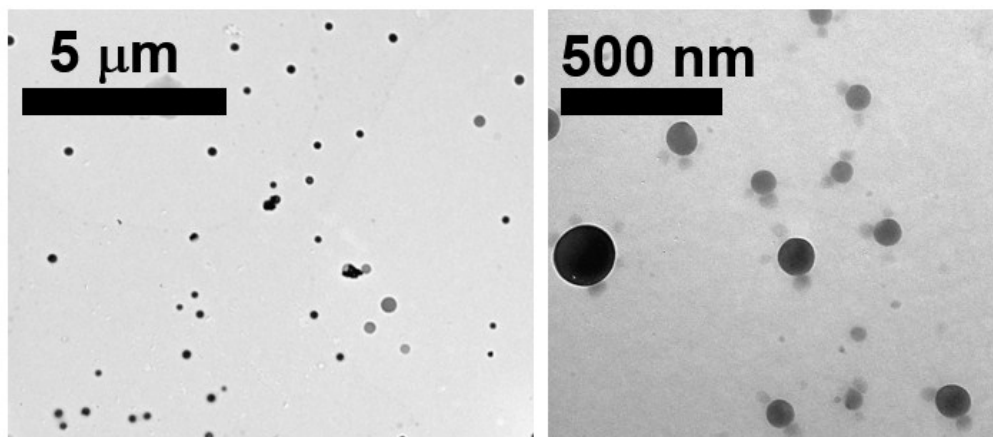


Figure S 4: Transmission electron microscopy (TEM) image of colloid 2. The particle size distribution is in line with DLS and SEM analyses. The sections shown are representative of the complete sample.

2.6 Atomic Force microscopy

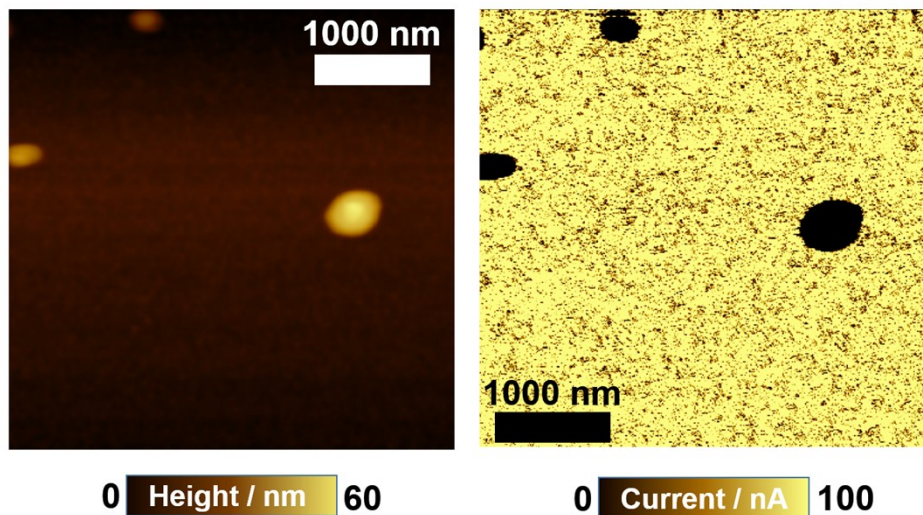


Figure S 5: Conductive atomic force microscopy (AFM) recorded at individual particle of colloid **2**. Left: topography and (right) conductive AFM, image recorded in air with a Ti-Pt-coated AFM probes; scan velocity of 0.34 line s⁻¹; applied voltage of 1.1 V.

2.7 X-ray photoelectron spectroscopy of **2**

X-ray photoelectron spectroscopy was performed for the determination of oxidation states in colloid **2**. For vanadium, the V(2p_{3/2}) level was found at 517.0 eV corresponding to fully oxidized vanadium centers.^{S2} The Mn(2p_{3/2}) level was found at 642.4 eV. Furthermore, the Mn(3s) peak was used for determination of the Mn oxidation states. The observed splitting between multiplet spin components of $\Delta E = 5.1$ eV suggests that colloid **2** contains Mn centers in oxidation state Mn^{III} and Mn^{IV}.^{S3, S4}

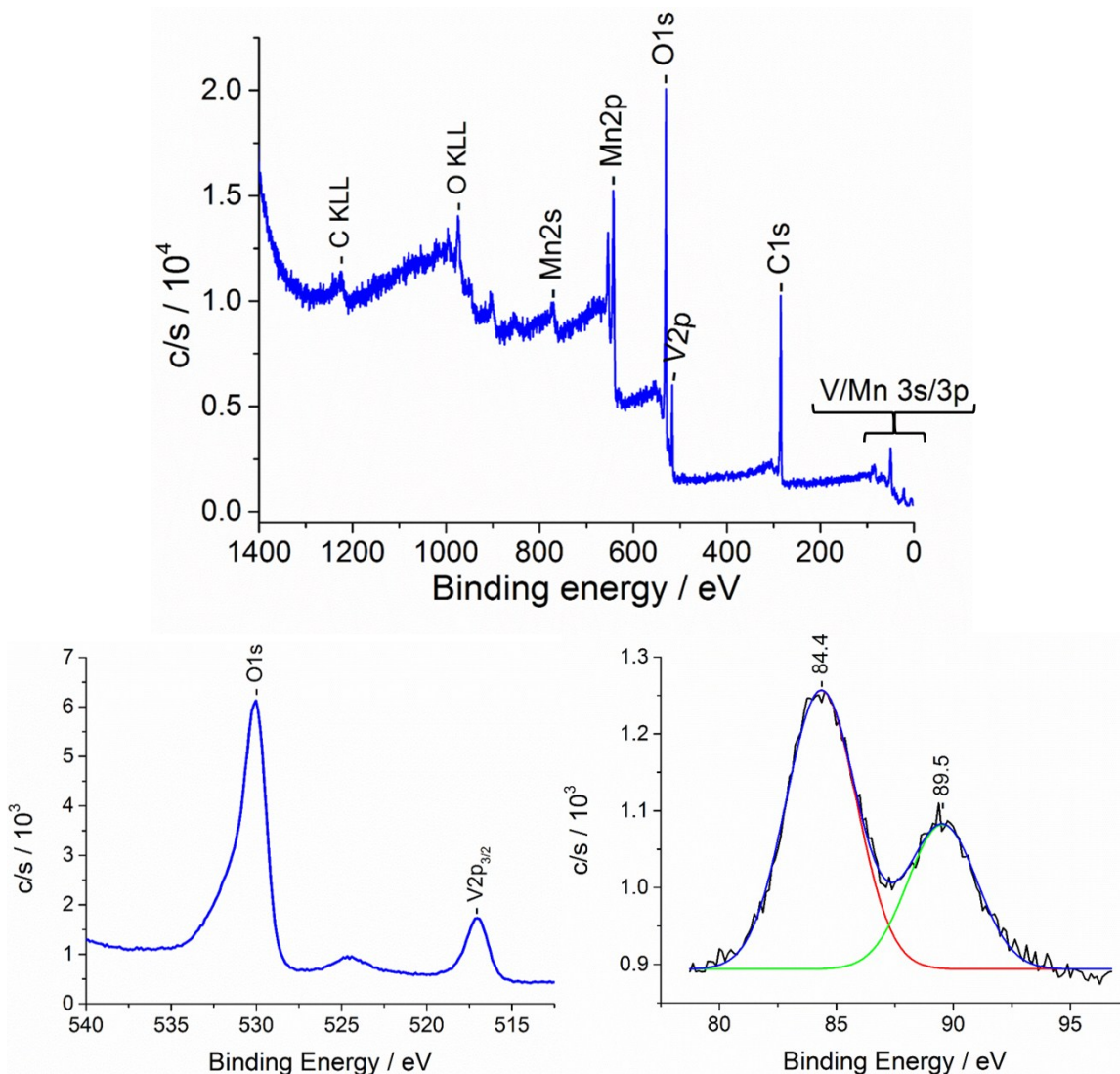


Figure S 6: Top: X-ray photoelectron spectrum of **2** (overview), indicating the presence of all expected elements. Mn, V and O are observed in an approximate ratio of 5:1:10. **Bottom left:** Detailed XPS spectrum of the O1s and V2p_{3/2} region. The observed binding energy of 517.0 eV for the V2p_{3/2} level corresponds to fully oxidized vanadium centers. **Bottom right:** Detailed XPS spectrum with peak fitting of the Mn3s region. The observed splitting ($\Delta E = 5.1$ eV) suggests mixed valent Mn centers in the oxidation states +III/+IV.

2.8 Flame-atomic absorption spectroscopic (FAAS) analysis of **2**

An aqueous sample of **2** (10 mg) was digested using *aqua regia* (10 ml). 1 ml of the clear solution was then diluted to 100 ml using demineralized H₂O, examined by flame atomic absorption spectroscopy and gave an approximate metal weight content of V: 0.89 mg/L : Mn 4.98 mg/L (i.e. V : Mn atomic ratio = 1 : 5.2). Within experimental error, this is in line with the assigned formula: VMn₅O₁₀ x ca. 6 H₂O x ca. 0.2 nBu₄N.

2.9 Nitrogen sorption analysis of **2**

Nitrogen sorption was used to investigate the specific surface area (BET method), specific pore volume and pore diameter (BJH method) of the colloidal particles:

Specific surface area:	240.40 m ² /g
Specific pore volume:	0.19 cm ³ /g
Average pore diameter:	3.1 nm

2.10 ATR-Infrared spectroscopy of **2**

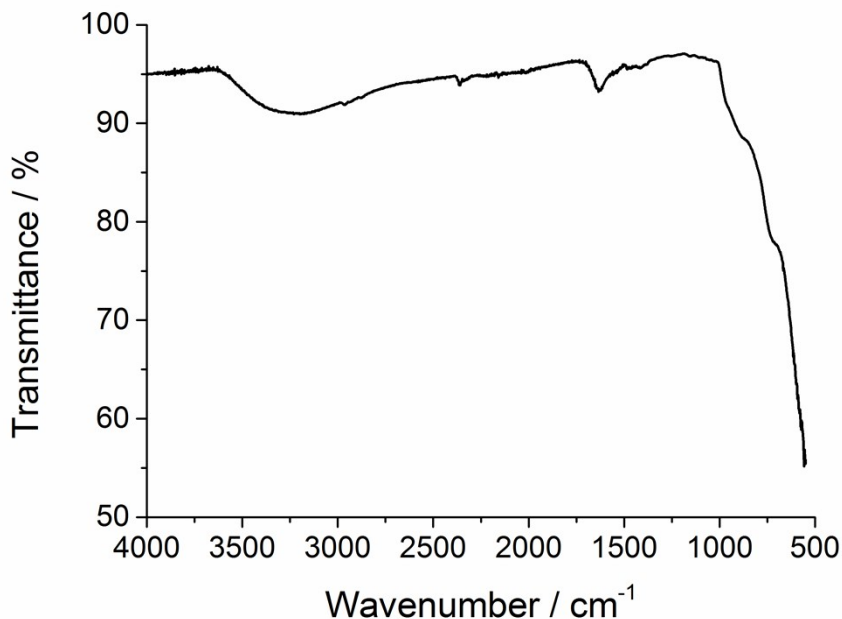


Figure S 7: ATR-Infrared spectroscopy of colloid **2** shows the Mn-O vibrations in the range of 500 – 700 cm⁻¹ and the water-bending (1500 – 1700 cm⁻¹) and –stretching bands (3000 – 3600 cm⁻¹).

2.11 Thermogravimetric analysis of **2**

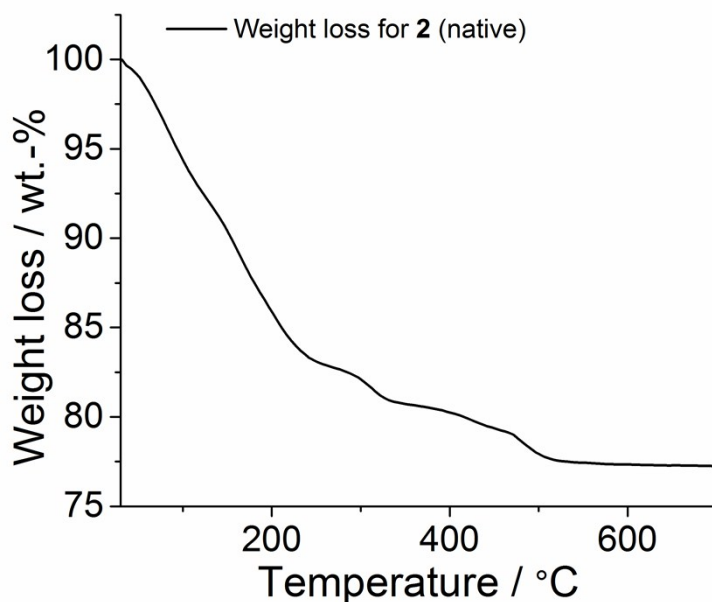


Figure S 8: Thermogravimetric analysis (TGA) of native colloid **2**. The weight loss between 100 – 180 °C is suggested to arise from the release of *ca.* six water molecules (exp.: 16.5 wt.-%, calcd. 16.8 wt.-%): The weight loss between 180 – 430 °C is suggested to arise from the loss of $n\text{Bu}_4\text{N}^+$ cations (*ca.* 0.2 cations per formula unit, exp.: 6.6 wt.-%, calcd.: 7.5 wt.-%). This is in line with CHN elemental analyses where a total organic content of 7.4 wt.-% is observed. The weight loss at *ca.* 500 °C is literature-known for related manganese oxides and is attributed to a release of oxygen due to the thermal reduction of Mn centres.^{S5}

2.12 Stability of colloid **2** under catalytic conditions

The stability of colloid **2** under catalytic conditions (pH = 0.6 - 0.9, $[\text{Ce}^{\text{IV}}] = 48 \text{ mM}$) was tested using dynamic light scattering. At low pH (pH < 2.4, adjusted using 1.0 M HNO_3) in the absence of cerium cations, precipitation of the colloid was observed by DLS and visually (see Fig. S 9). In contrast, when cerium cations are present in the solution ($[\text{Ce}^{\text{IV}}] = 48 \text{ mM}$), no change in particle size is observed by DLS measurements and no precipitation is observed, suggesting a stabilizing effect by the cerium cations.

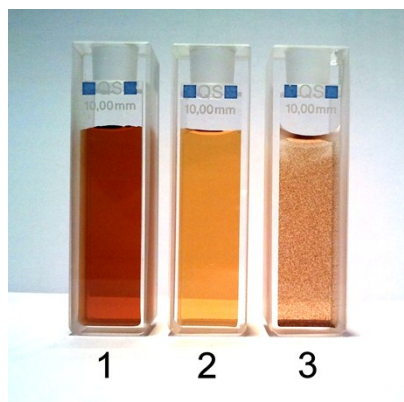


Figure S 9: Photographs of solutions of colloid **2**. Picture 1: colloid **2** in pure water ($[I] = 0.5 \text{ g/L}$, pH 5.4). Picture 2: colloid **2** under reaction conditions ($[Ce^{IV}] = 48 \text{ mM}$, pH 0.7), no precipitation is observed. Picture 3: colloid **2** adjusted to pH = 0.7 using 1.0 M HNO_3 ; precipitation is observed. Reaction time: ca. 60 min.

2.13 Clark-electrode setup for catalytic oxygen evolution measurements

The Clark-electrode (black) is sealed with two O-rings (black lines) and a gas-tight PTFE cap (white) in a sealed three-necked flask, see Fig. S 10. Two septa (grey) are attached to the smaller necks of the flask. *Via* cannulas, deoxygenated solutions or dried nitrogen gas can be introduced into the inert-atmosphere reactor. The typical reaction volume used was 5 - 10 ml.

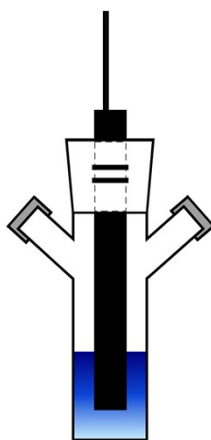


Figure S 10: Scheme of the Clark-electrode setup.

2.14 Chemical water oxidation catalysis by colloid 2

Description of a typical water oxidation experiment of colloid 2:

Colloid 2 was obtained by dissolving compound 1 (0.2 g/L; 0.5 g/L; 1.0 g/L) in 5.0 ml de-ionized water. The solution was transferred into the Clark-electrode vessel and deoxygenated (for ca. 15 minutes) with dry nitrogen until oxygen levels were below the Clark electrode detection limit (2.5 μM). A stock solution of $\text{Ce}(\text{NO}_3)_4$ ($[\text{Ce}(\text{NO}_3)_4] = 1.0 \text{ M}$) was deoxygenated and 250 μl of this solution (final $[\text{Ce}(\text{NO}_3)_4] = 48 \text{ mM}$) was injected into the Clark-electrode vessel *via* cannula and syringe. Oxygen evolution was measured and recorded as a function of time (see Fig. S 11). As a reference, Mn_2O_3 was finely ground and the solution thereof ($c = 1.0 \text{ g/L}$) was sonicated for 20 min prior to oxidant addition.

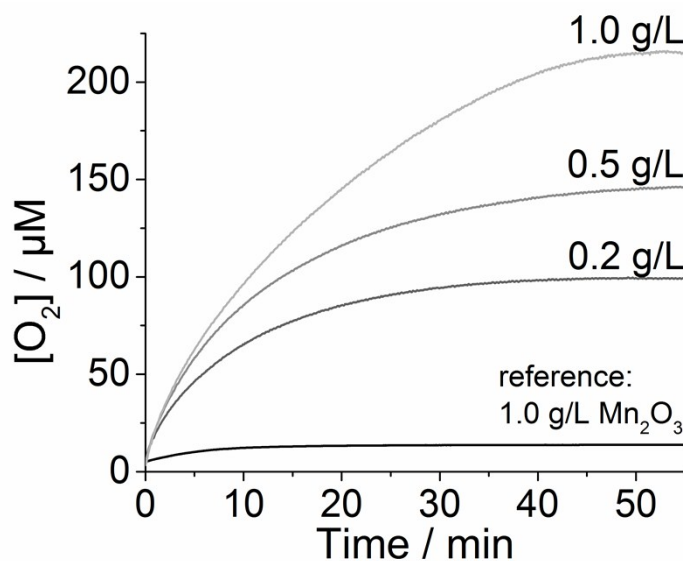


Figure S 11: Oxygen evolution by colloid 2. *In situ* oxygen evolution measurements of oxygen evolution upon addition of cerium(IV) nitrate (1.0 M, 250 μl) to solutions of colloid 2 (based on 0.2 g/L, 0.5 g/L, 1.0 g/L of 1 dissolved in water). For comparison, oxygen evolution of a 1.0 g/L solution of Mn_2O_3 under identical experimental conditions is shown (black).

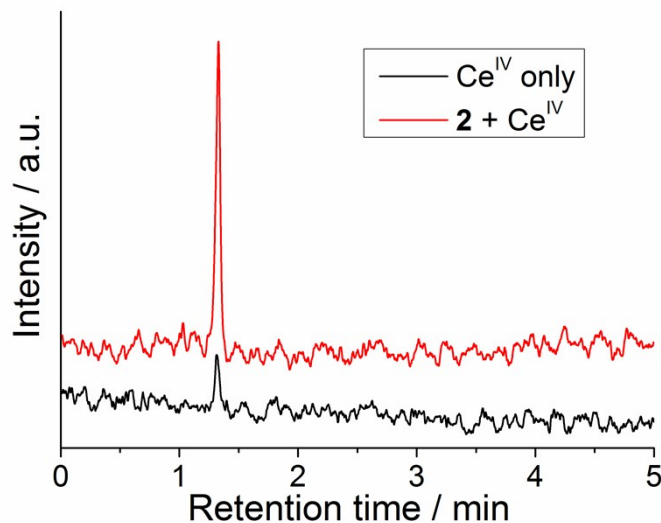


Figure S 12: Gas-chromatographic determination of oxygen in the gas phase of a reaction mixture after the addition of Ce^{IV} to water (black) and to a solution containing **2** (red).

2.15 Post-catalytic investigations of **2**

For bulk analysis of **2** after catalysis, the colloidal particles were precipitated from aqueous solution by the addition of an excess of acetone. The mixture was allowed to stand for one day followed by prolonged centrifugation (4400 rpm). The precipitate obtained was washed with acetone (3x) and was dried.

X-ray photoelectron spectroscopy:

X-ray photoelectron spectroscopy was performed for the determination of oxidation states in colloid **2** after the addition of $\text{Ce}(\text{IV})$. The spectrum indicates the presence of Mn, V, Ce, O and C. For vanadium, the $\text{V}(2p_{3/2})$ level was found at 517.3 eV corresponding to fully oxidized vanadium centers.^{S2} The $\text{Mn}(2p_{3/2})$ level was found at 642.5 eV. Furthermore, the $\text{Mn}(3s)$ peak was used for determination of the Mn oxidation states. The observed splitting between multiplet spin components of $\Delta E = 5.3$ eV suggests that colloid **2** contains Mn centers in oxidation state Mn^{III} and Mn^{IV} after the addition of $\text{Ce}(\text{IV})$.^{S3, S4} In addition, cerium cations were observed in the precipitated colloids after $\text{Ce}(\text{IV})$ addition. The $\text{Ce}3d$ region shows a total of eight peaks, which can

be assigned to a mixture of Ce(IV) and Ce(III) cations based on Ce3d envelope comparison and peak fitting. The binding energy peaks located at 882.8, 888.9, 898.7, 901.0, 907.4 and 917.1 eV are characteristic for tetravalent Ce. The binding energy peaks at 885.7 and 902.7 eV indicate the presence of minor amounts of trivalent cerium in the sample.^{S6}

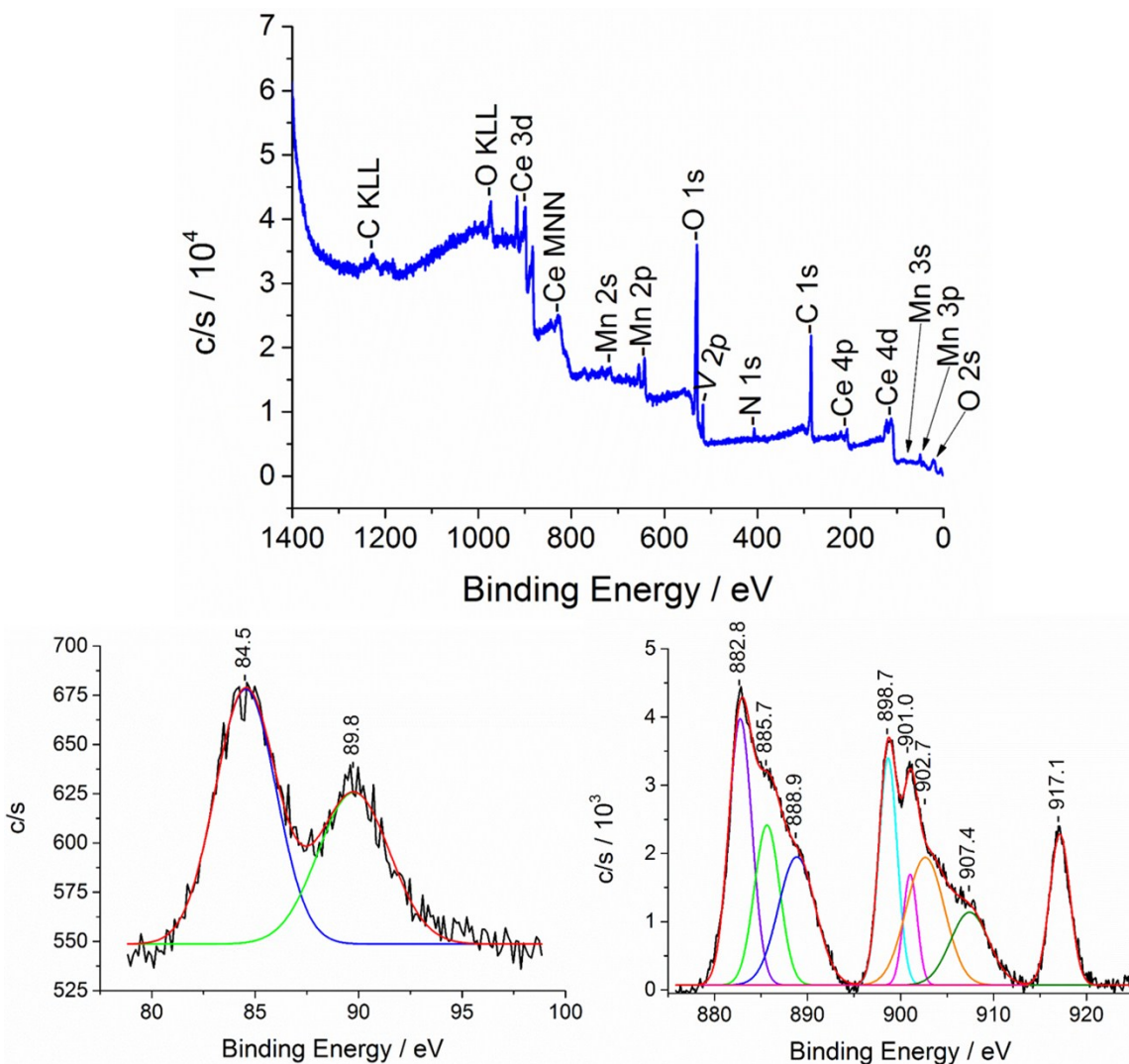


Figure S 13: **Top:** X-ray photoelectron spectrum of **2** after Ce(IV) addition (overview), indicating the presence of Mn, V, Ce and O. **Bottom left:** Detailed XPS spectrum with peak fitting of the Mn3s region. The observed splitting ($\Delta E = 5.3$ eV) suggests mixed valent Mn centers in the oxidation states +III/+IV. **Bottom right:** Detailed XPS spectrum with peak fitting of the Ce3d region. The observed binding energy values correspond to tetravalent Ce as well as a minor amount of Ce(III).

Comparative infrared spectroscopy:

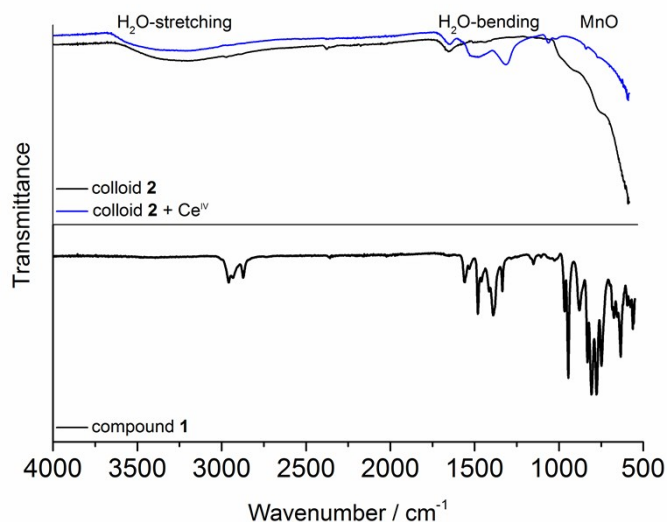


Figure S 14: Comparative ATR-infrared spectroscopic studies of the colloidal particles before and after water oxidation catalysis (top) and the precursor compound **1**. The colloidal particles show the expected Mn-O vibrations (500 – 700 cm⁻¹) as well as water stretching (3000 – 3600 cm⁻¹) and bending bands (3000 – 3600 cm⁻¹). In addition to Mn-O and V-O modes, further bands in the range of 1000 – 1500 cm⁻¹ might originate from Ce-O modes. This is in accordance to previously reported bands of cerium oxides.^{S7}

Thermogravimetric analysis:

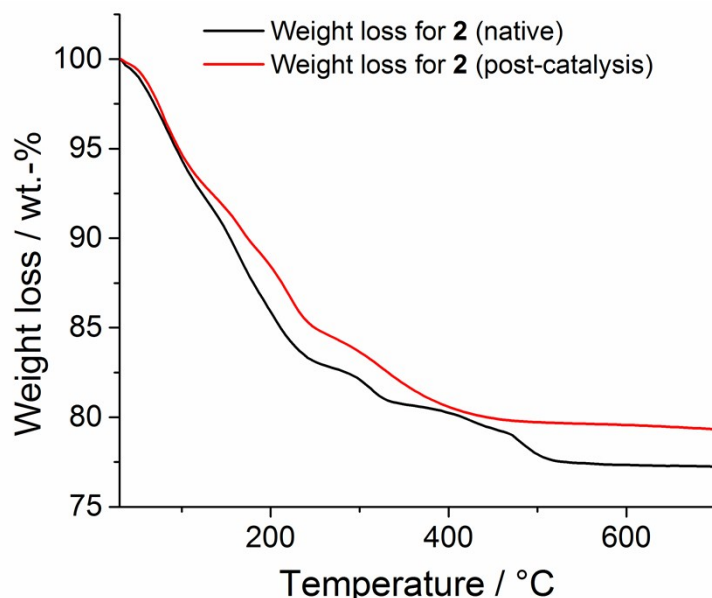


Figure S 15: Comparative thermogravimetric analysis (TGA) of colloid **2** before and after catalysis. Note that in the temperature range up to ca. 400 °C, similar thermogravimetric behavior is noted.

2.16 Recovery and re-use of colloid **2**

To understand whether colloid **2** can be recovered from solution and re-dispersed, the following procedure was performed: To an aqueous solution of colloid **2** ($[1] = 0.5$ g/L, average particle size: ca. 69 nm) an acetone/water mixture (1:1, v:v) was added. The reaction mixture was allowed to stand for 4 days to complete precipitation. The resulting precipitate was filtered off by centrifugation and was thoroughly washed several times with acetone. Then the sample was dried in the oven at 120 °C for 30 min. After cooling to room-temperature, the solid sample was re-dissolved in 5.0 ml of deionized water. DLS analysis of the non-filtered solution gave an average particle size of 78 nm (see Fig. S 16). Oxygen evolution measurements using standard conditions ($[\text{Ce}(\text{NO}_3)_4] = 1.0$ M, $V = 250$ μl) showed that the final oxygen concentration was 75 μM (black line). A native sample of **2** under identical oxygen evolution conditions gave final oxygen concentration of 146 μM (red line). Catalytic oxygen evolution of the precipitated and re-dissolved samples shows a drop of ca. 49 %, see Fig. S 16.

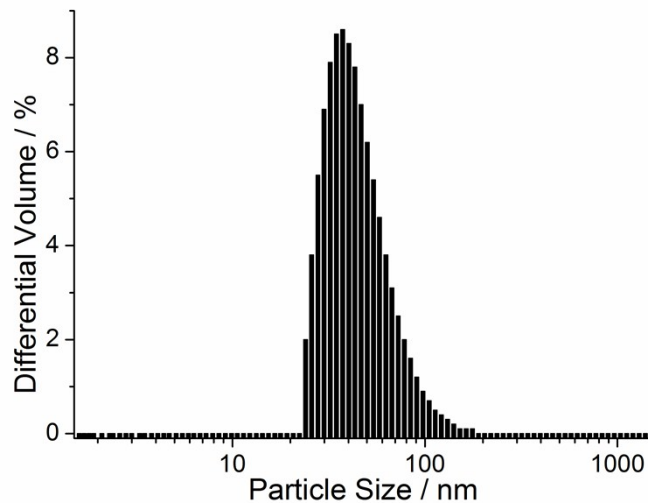


Figure S 16: Volume distribution of re-dissolved colloid **2** gives particles between ca. 20 and 180 nm and an average particle size of 78 nm (native particle size: 69 nm, note: particle size: logarithmic scale).

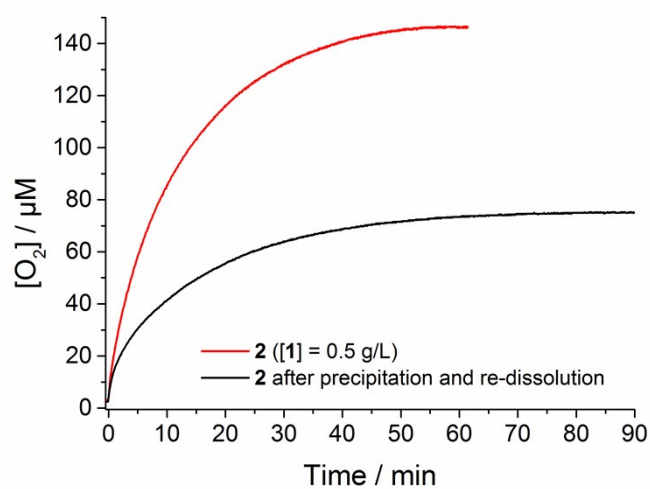


Figure S 17: Time-dependent oxygen evolution by a precipitated and re-dissolved sample of **2** (black line). A native sample of **2** under identical conditions shows higher oxygen evolution (red line). The oxygen yield is decreased by ca. 49 %.

Table S1: Water oxidation rates of manganese oxide based WOCs.

Compound	Initial WOC rate [mmol _{O₂} mol _{Mn} ⁻¹ h ⁻¹]
Ca0.00 ^{S8} (synthetic birnessite)	250
Ca0.21 ^{S8} (synthetic birnessite)	1175
T400 ^{S8} (synthetic birnessite)	3000
KB ^{S5b} (potassium birnessite)	2968
KB@MF ^{S5b} (birnessite/Mn ferrite nanocomposite)	3400
CaB@MF ^{S5b} (birnessite/Mn ferrite nanocomposite)	3900
This work	1490 (± 150)

3 Literature references

- S1 B. Schwarz, J. Forster, M. K. Goetz, D. Yücel, C. Berger, T. Jacob and C. Streb, *Angew. Chem. Int. Ed.*, 2016, **55**, 6329 – 6333.
- S2 E. Hryha, E. Rutqvist and L. Nyborg, *Surf. Interface Anal.*, 2012, **44**, 1022 – 1025.
- S3 M. Oku, K. Hirokawa and S. Ikeda, *J. Electron Spectros. Relat. Phenomena*, 1975, **7**, 465 – 473.
- S4 G. K. Wertheim, S. Hüfner and H. J. Guggenheim, *Phys. Rev. B*, 1973, **7**, 556 – 558.
- S5 a) D. L. Bish and J. E. Post, *Am. Mineral.*, 1989, **74**, 177 – 186; b) G. Elmacı, C. E. Frey, P. Kurz and B. Zümreoğlu-Karan, *J. Mater. Chem. A*, 2016, **4**, 8812 – 8821.
- S6 E. Bêche, P. Charvin, D. Perarnau, S. Abandes and G. Flamant, *Surf. Interface Anal.*, 2008, **40**, 264 – 267.
- S7 S. Thakur and P. Patil, *Sens. Actuator B Chem.*, 2014, **194**, 260 – 268.
- S8 C. E. Frey, M. Wiechen and P. Kurz, *Dalton Trans.*, 2014, **43**, 4370 – 4379.